Pavlo HERASYMENKO

Institute of Electrodynamics of the National Academy of Sciences of Ukraine

doi:10.15199/48.2021.05.07

Combined PS-PDM control method for voltage-source series-resonant inverter

Abstract. *This paper proposes a new control method for a voltage-source series-resonant inverter (SRI) of the induction heating system. The proposed method of control is based on combining the phase-shift (PS) and pulse-density-modulation (PDM) controls. The main feature of this control method is that the current regulation for pulse density in the range from 0.5 to 1 is provided by only the traditional PDM control and in the range from 0 to 0.5 – with the PS control and constant density equal to 0.5 of the PDM control. Theoretical analysis shows that using the proposed control method can reduce the peak-to-peak current fluctuation and increase the minimum peak current of the SRI, compared with the traditional PDM control. The results of numerical computations are in good agreement with the results of simulations. Experiments were carried out to confirm the practical applicability of the proposed control method for series-resonant inverters for induction heating application.*

Streszczenie. *W artykule zaproponowano nową metodę sterowania falownikiem rezonansowym szeregowym ze źródłem napięcia (SRI) systemu ogrzewania indukcyjnego. Proponowana metoda sterowania opiera się na połączeniu sterowania przesunięciem fazowym (PS) i modulacji gęstości impulsów (PDM). Główną cechą tej metody sterowania jest to, że regulację prądu dla gęstości impulsów w zakresie od 0,5 do 1 zapewnia tylko tradycyjne sterowanie PDM, a zakresie od 0 do 0,5 - ze sterowaniem PS i stałą gęstością. Analiza teoretyczna pokazuje, że zastosowanie proponowanej metody sterowania może zmniejszyć wahania prądu międzyszczytowego i zwiększyć minimalny prąd szczytowy SRI w porównaniu z tradycyjnym sterowaniem PDM.* (***Połączona metoda sterowania PS-PDM dla falownika rezonansowego szeregowego ze źródłem napięcia***)

Keywords: control method, current fluctuation, induction heating, pulse-density modulation, phase-shift control, series-resonant inverter.
Słowa kluczowe: sterowanie przesunięciem fazy PS, sterowanie gęstością impulsów PDM, nagrzewanie indukcyjne.

Introduction

A voltage-source series-resonant inverter (SRI) is well used for induction heating systems because of its simple power circuit topology and because many different control techniques are suitable to regulate its output current or power [1-11]. Various control techniques have been proposed to provide soft-switching operation modes of SRI transistors. In recent years, one of the frequently mentioned control techniques is pulse-density modulation (PDM) [8-12]. This technique makes it possible to achieve zero-voltage and quasi-zero-current switching (ZVS and ZCS) operations of the SRI transistors. However, the use of PDM leads to peak-to-peak fluctuations of the SRI output current, and the lower the value of the quality factor of the series-resonant circuit, the higher the fluctuation. This can be a serious problem, as at low values of the output current of the SRI, transistors' commutation can occur under NON-ZVS conditions.

Various enhanced PDM techniques have been proposed to reduce the peak-to-peak current fluctuation [11-14]. Compared to the traditional PDM control technique, in which durations of an injecting interval and a free-wheeling interval are multiple of the SRI output voltage period, the enhanced PDM techniques operate with durations that are multiple to half-period of the SRI output voltage. In [13] an enhanced PDM technique is proposed, according to which only the duration of the free-wheeling interval is a multiple of the SRI output voltage period. This makes it possible to achieve smaller fluctuations in comparison to the traditional PDM control technique for the same pulse density. In [14-16], the authors proposed the enhanced PDM technique, according to which both the injection interval and the free-wheeling interval are multiple of the half-period of the SRI output voltage. This technique provides smaller fluctuations compared to the traditional PDM control technique and the enhanced PDM control technique proposed in [13]. But in this case, the SRI output voltage contains a DC component. To avoid the appearance of the DC component on the primary side of the matching transformer of the induction heating system, a blocking capacitor is required, and it should be paid careful attention to the choice of its capacity. Thus, this PDM technique is convenient when there is no need to use the matching transformer in the induction heating system.

Also, modular converters topologies with PDM control have been proposed to reduce the peak-to-peak current fluctuation [16-18]. The use of the converters that have several identical channels with the interleaved control to reduce a current/voltage ripple is well known [19-20]. The more channels in the converter, the fewer the fluctuation. But the modular converter must have at least two channels, which is not always expedient in the case of low-power converters. In [21] the authors proposed the extended topology of the SRI, which combines the topologies of a half-bridge inverter and a full-bridge inverter. This converter topology has fewer transistors and provides the same peak-to-peak current fluctuations in comparison to the two-channel modular converter with the interleaved or stepped PDM controls. However, this topology has its drawbacks: the reverse recovery problem of anti-parallel diodes; not evenly discharging the capacitors of the half-bridge inverter topology. Still, there is necessary to have more transistor in comparison to a conventional full-bridge inverter topology.

Combining PDM control with other control techniques makes it is possible to reduce the fluctuation. One of the control techniques which is reasonable to use with PDM is the phase-shift (PS) control. Because the phase-shift-controlled SRI operates at the frequency close to the operating frequency of the pulse-density modulated SRI, so it is easy to combine them. Hybrid PS-PDM power control is presented in [22], in which the PS and PDM control techniques operate simultaneously, which means that the phase-shift control is used between PDM patterns to provide more continuous power regulation, which in general does not allow to reduce the current fluctuations. Also, during a working process, which is presented in [22], the output voltage of the SRI contains a DC component. In [23], among other things, the author also discusses a tuning system which can simultaneously utilize pulse-density-modulation and phase-shift controls, which leads to more continuous power regulation, compared to the traditional PDM. However, the output frequency could be three and more times less than the operating frequency of the traditional PDM SRI. Thus, in this case, the matching transformer will be significantly larger.

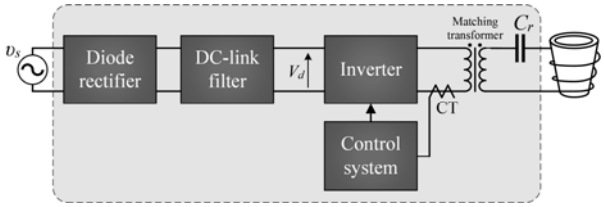

Fig.1. Typical power system configuration of an induction heating system

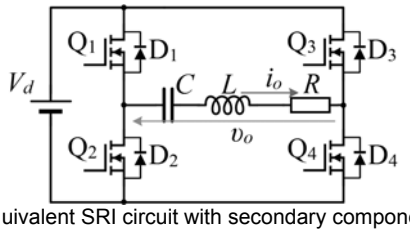

Fig.2. Equivalent SRI circuit with secondary components reflected to the primary side

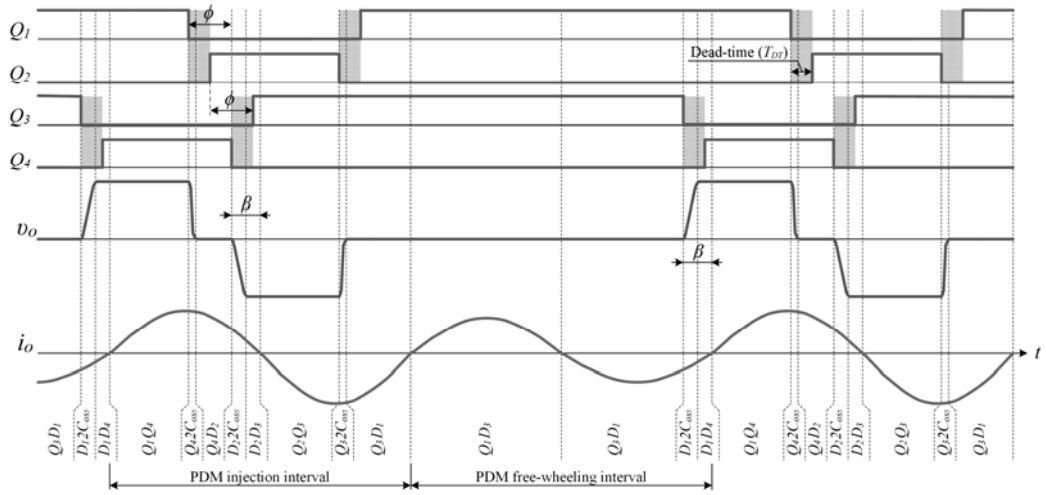

Fig.3. Switching sequence in the proposed combined PS-PDM control method

In order to reduce the peak-to-peak current fluctuation and increase the minimal peak current, especially at a low value of the quality factor, this paper proposes a combined PS-PDM control method for a series-resonant inverter in which current regulation is provided by the traditional PDM control only with the free-wheeling interval no more than one period of the SRI output voltage. In such a way, the minimal pulse density of PDM is 0.5. If this density is not sufficient to limit or regulate the output current of the SRI, the regulation current is provided by the PS control simultaneously with the active PDM pattern. To determine the performance of the proposed PS-PDM control method compared to the traditional PDM, numerical computations with simulation were performed. The experimental waveforms obtained on an experimental setup have confirmed the feasibility of the proposed control.

SRI with the combined PS-PDM control method

A. Circuit Description and Principle of Operation

A typical system configuration of an induction heating system consists of a diode rectifier, a DC-link filter, a high-frequency resonant inverter, a matching transformer, a resonant capacitor, and a control system (Fig. 1). An induction coil of the induction heating system with a workpiece can be represented as a series connection of an equivalent inductor and an equivalent resistor.

Fig. 2 shows an equivalent SRI circuit with secondary components reflected to the primary side. The topology of the SRI is full-bridge with four MOSFETs Q_1-Q_4.

The SRI operates slightly above the resonant frequency. Thus, the output current i_O of the SRI legs the output square-wave voltage v_O of the SRI. Body diodes D_1-D_4 of the transistors Q_1-Q_4, respectively, conduct current once the parasitic capacitances of the transistors are discharged. During these diodes' conduction intervals, the transistors are turned-on at zero voltage. Thus, there is no problem with the transistors overlapping and the reverse-recovery problem of the diodes. The phase portion β, where the voltage v_O and current i_O are in the opposite direction, is essential to determine the ZVS operation (Fig. 3).

The switching modes of the voltage-source series-resonant inverter with the PS and PDM control techniques are well known and widely described in the literature [1], [8]. Fig. 3 illustrates the switching sequence and waveforms of the proposed combined PS-PDM control method. In this case of combining PS and PDM controls, the current regulation is provided by PDM control only with the free-wheeling interval no more than one period of the SRI output voltage. In such a way, the minimum value of the pulse density of PDM is 0.5. If this density is not sufficient to limit or regulate the output current, the current regulation is provided by PS control by changing phase-shift ϕ between the control signals Q_1/Q_4 and Q_2/Q_3 of the transistors Q_1-Q_4 simultaneously with the active PDM pattern. Thus, within the PDM injection interval, there is present the free-wheeling interval caused by PS control (stages D_2/Q_4 and D_1/Q_3 in Fig. 3). There is no DC component in the waveform of the output voltage v_O. Thus, it is not necessary to use the blocking capacitor on the primary side of the matching transformer.

B. Analysis of Output Current

Fig. 4 depicts waveforms of i_O and v_O under the assumption that the capacitance of the MOSFET's output capacitor is small compared to the resonant capacitor, thus its effect on the output current and voltage during the switching transition is small and negated.

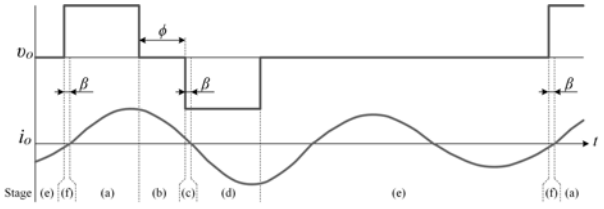

Fig. 4. Waveforms of i_O and v_O under the assumption that the capacitance of the MOSFET's output capacitor is small compared to the resonant capacitor

Assuming the initial values of the current $i_O = I_{0x}$ and the resonant capacitor voltage $\upsilon_C = V_{0x}$, where x is the relevant stage under review; the output current $i_O(t)$ and the voltage $\upsilon_C(t)$ across the resonant capacitor C in the time domain are given by

$$(1)\qquad i_O(t) = I_{0x}\cos(\omega_d t)e^{-\frac{R}{2L}t} + \frac{-\frac{RI_{0x}}{2} + \mathrm{sgn}(V_d)V_d - V_{0x}}{L\omega_d}\sin(\omega_d t)e^{-\frac{R}{2L}t},$$

$$(2)\qquad \upsilon_C(t) = \mathrm{sgn}(V_d)V_d + \left(V_{0x} - \mathrm{sgn}(V_d)V_d\right)\cos(\omega_d t)e^{-\frac{R}{2L}t} + \left(\frac{I_{0x}}{\omega_d C} + \frac{R}{2L\omega_d}\left(V_{0x} - \mathrm{sgn}(V_d)V_d\right)\right)\sin(\omega_d t)e^{-\frac{R}{2L}t}$$

where: ω_d is the damped frequency, and $\mathrm{sgn}(V_d)$ is the sign function of V_d are given by

$$(3)\qquad \omega_d = \sqrt{\frac{1}{LC} - \frac{R^2}{4L^2}},$$

$$(4)\qquad \mathrm{sgn}(V_d) = \begin{cases} 1 & \text{for stages (a) and (f);} \\ 0 & \text{for stages (b) and (e);} \\ -1 & \text{for stages (c) and (d).} \end{cases}$$

In fig. 4 are shown six stages, but since the voltage doesn't change sign at stages (f) and (a), as well as (c) and (d), the output current $i_O(t)$ and voltage $\upsilon_C(t)$ can be mathematically described for four stages of the voltage υ_O (Fig. 5):

$$(5)\qquad \mathrm{sgn}(V_d) = \begin{cases} 1 & \text{for stages (a);} \\ 0 & \text{for stages (b) and (d);} \\ -1 & \text{for stages (c).} \end{cases}$$

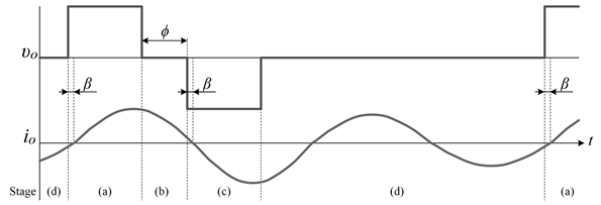

Fig.5. Four stages of υ_O, in contrast to Fig. 4

The duration of the phase portion β during the stages (f) and (c) in Fig. 4 or stages (a) and (c) in Fig. 5 differs because of the different values of the SRI output current at the beginning of these stages. In the case when the zero-crossing moments of i_O and υ_O are synchronized by a frequency-tuning system at the beginning of the stages (d) in Fig. 4 and (c) in Fig. 5, the duration of these stages is 0.

Solutions (1) and (2) are very difficult to analyze because each equation requires an initial condition, the solution of which is a function of the previous stage equation. The analysis of these equations can be simplified by using numerical computation software such as Mathcad or MATLAB.

Table 1. Parameters of numerical computation

	ϕ	V_d [V]	R [Om]	L [uH]	C [uF]	Q	$f_O = 1/T_O$ [Hz]
Fig. 6,a	50°	1	0.11132	2.2	7.1	5	43674
Fig. 6,b	50°	1	0.11132	2.2	7.1	5	42272

Fig. 6 depicts waveforms of i_O and υ_O which have been obtained as a result of numerical computation of (1), (2), and (5) in Mathcad at the same parameters but different values of the operating frequency f_O. The values of the used parameters for numerical computation are presented in Table 1.

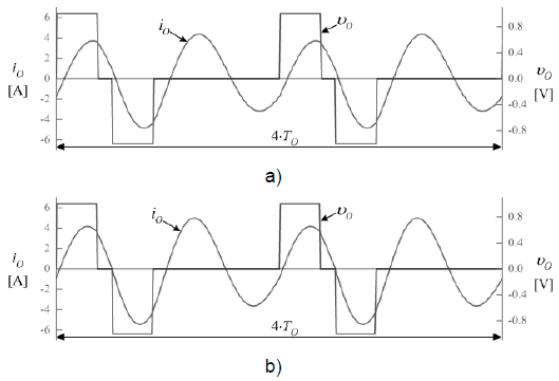

Fig. 6. Waveforms of i_O and υ_O obtained as a result of numerical computation: a) f_O = 43674 (duration of stage (c) is 0), b) f_O = 42272.

Fig. 6,a shows the case of the current i_O lagging from the voltage υ_O, so the switching of transistors occurs with ZVS. In the waveforms shown in Fig. 6,b, the voltage and current have one common zero-point, which means that at this point the duration of the phase portion β is equal to 0. These two cases are obtained for the same parameter values, except the operating frequency (Table 1). Thus, the waveforms of i_O and υ_O depend on the operation of a phase-locked loop system and the desired phase-shift that the phase-locked loop system sets/adjusts between i_O and υ_O.

Comparison of Simulation and Numerical Computation results

To verify the results of numerical computations, validation was performed using simulation in the MATLAB/Simulink environment. Fig. 7 shows the circuit model used for simulation. During simulation and numerical computation, the operation frequency was set to provide waveforms of i_O and υ_O as is shown in Fig. 6,b.

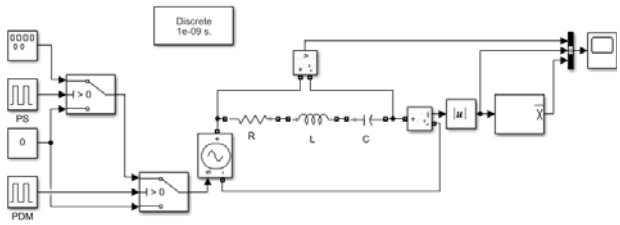

Fig. 7. Circuit model used for simulation

Fig. 8. shows the numerically calculated with Mathcad and obtained as a result of simulation with MATLAB/Simulink relations between the normalized values of the minimum peak current $I^*_{p(\min)}$ and the average rectified current I^*_{avg} for different values of the quality factor Q. The normalized values $I^*_{p(\min)}$ and I^*_{avg} are given by

$$(6)\qquad I^*_{p(\min)} = \frac{I_{p(\min)}(\phi, D)}{I_p},$$

$$(7)\qquad I^*_{avg} = \frac{I_{avg}(\phi, D)}{I_{avg}}$$

where: I_p and I_{avg} are the values of the peak current and the average rectified current in the case of the pulse density D = 1 and phase-shift ϕ = 0, respectively, and $I_{p(\min)}$ and I_{avg} are the values of the minimum peak current and the average rectified current under set values of ϕ and D, respectively.

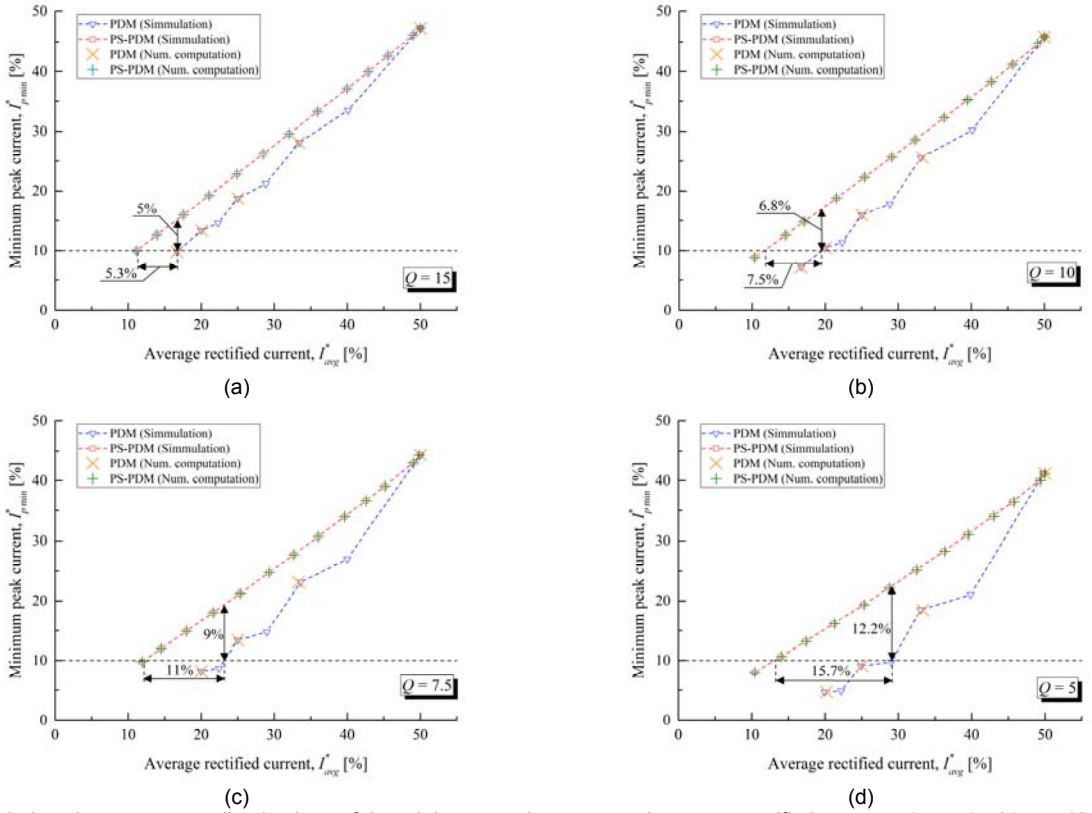

Fig. 8. Relations between normalized values of the minimum peak current and average rectified current: a) Q = 15, b) Q = 10, c) Q = 7.5, and d) Q = 5.

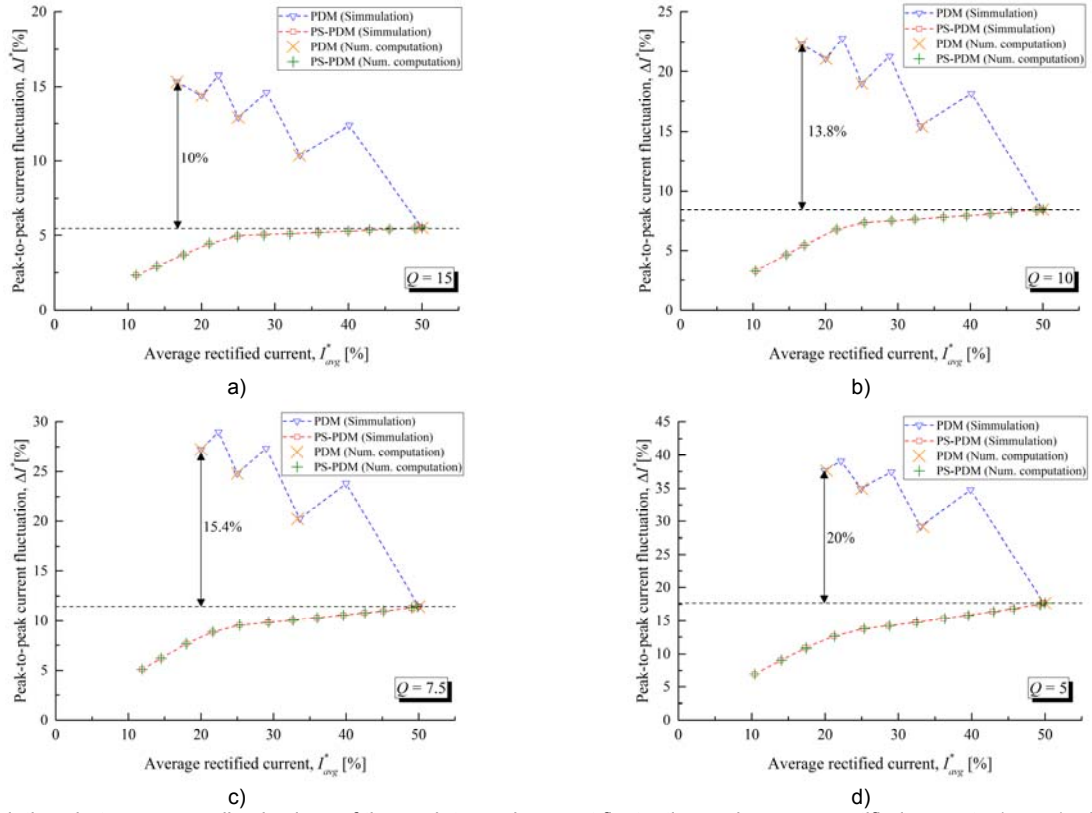

Fig. 9. Relations between normalized values of the peak-to-peak current fluctuation and average rectified current: a) Q = 15, b) Q = 10, c) Q = 7.5, and d) Q = 5

The effectiveness of the proposed PS-PDM control in comparison with the traditional PDM control can be evaluated by two criteria: 1) how much it is possible to increase the value of the minimum peak current; 2) how much it is possible to expand the regulation range of the average rectified current. The comparison was made at the level of 10% of the minimum peak current. As can be seen in Fig. 8, in the regulation range of the average rectified current from 10% to 50%, at high values of Q there are no significant differences between the values of the minimum

peak current depending on the PDM and PS-PDM controls. It is possible to increase the value of the minimum peak current up to 5% and 6.8% or extend the regulation range by 5.3% and 7.5% at $Q = 15$ and $Q = 10$, respectively. But, at low values of Q, it is possible more significant to increase the value of the minimum peak current up to 9% and 12.2% or extend the regulation range by 11% and 15.7% at $Q = 7.5$ and $Q = 5$, respectively.

Fig. 9 shows a similar relation between the normalized values of the peak-to-peak current fluctuation ΔI^* and the average rectified current I^*_{avg} for different values of the quality factor Q. The normalized value of ΔI^* is given by

$$\Delta I^* = \frac{I_{p(\max)}(\phi, D) - I_{p(\min)}(\phi, D)}{I_p} \tag{8}$$

where: $I_{p(\max)}$ is the maximum value of the peak current under set values of ϕ and D, respectively.

As can be seen in Fig. 9, the peak-to-peak fluctuation of i_O can be significantly reduced (up to 20% at Q = 5 from the point of I^*_{avg} (D = 0.5). This is important because the fluctuation affects the correct measurement of the average rectified value of i_O and the provision of ZVS modes of the transistors.

The calculated relative error value of the maximal deviation between the numerically calculated and obtained as a result of simulation values of the minimum peak current and the peak-to-peak current fluctuation is no more than 0.09%, which confirms the correctness of (1), (2) and (5), as well as the possibility of using these equations for analyzing the output current of the SRI with the proposed control method.

Both numerical computation and simulation showed that with deep regulation of the average rectified current, the operating frequency increased by 24% at Q = 5. Such an increase in operating frequency is insignificant, which confirms the possibility of combining the PS and PDM controls in the case of the described above method.

Experimental Results

To confirm that the SRI can function with the proposed combined PS-PDM control method, the proposed control method has been verified on the experimental setup of the SRI of the induction heating system (Fig. 10). The control system is based on the 32-bit STM microcontroller of F7 line (STM32F746ZET6). Fig. 11 shows some waveforms of i_O and v_O, obtained in the course of experimental research. Fig. 11,a shows waveforms of i_O and v_O in the case when the phase-shift ϕ equals zero and the pulse density is 0.5. Figs. 11,b and 11,c show waveforms of i_O and v_O for two different values of ϕ: Fig. 11,b – the value of ϕ > 0, and Fig. 11,b – the value of ϕ > than the value of ϕ of the case Fig.11,b.

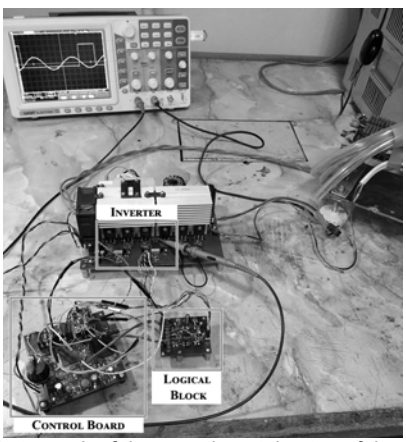

Fig. 10. Photograph of the experimental setup of the SRI

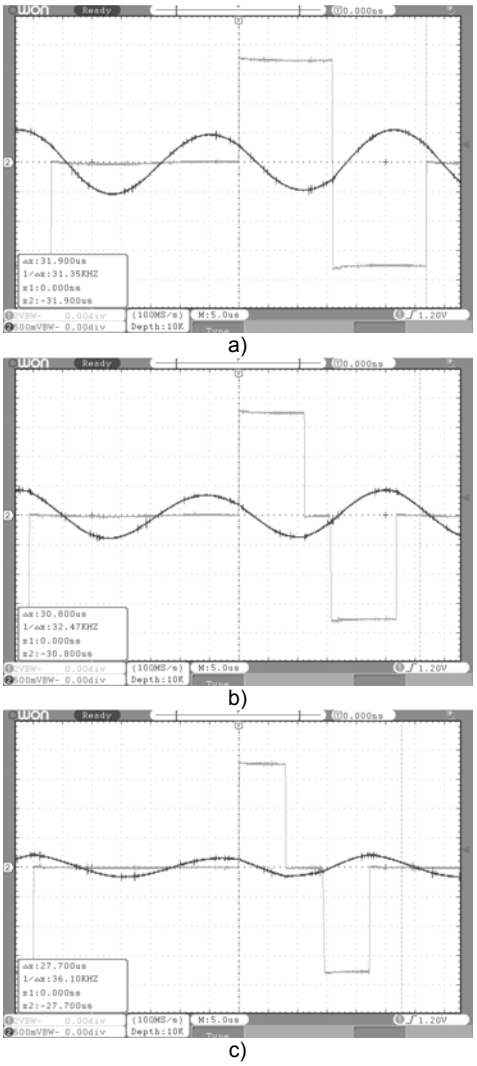
a)

b)

c)

Fig. 11. Waveforms of the voltage v_O and current i_O: a) in the case of ϕ = 0; b) in the case of ϕ > 0; c) in the case of ϕ more than ϕ of the case (b)

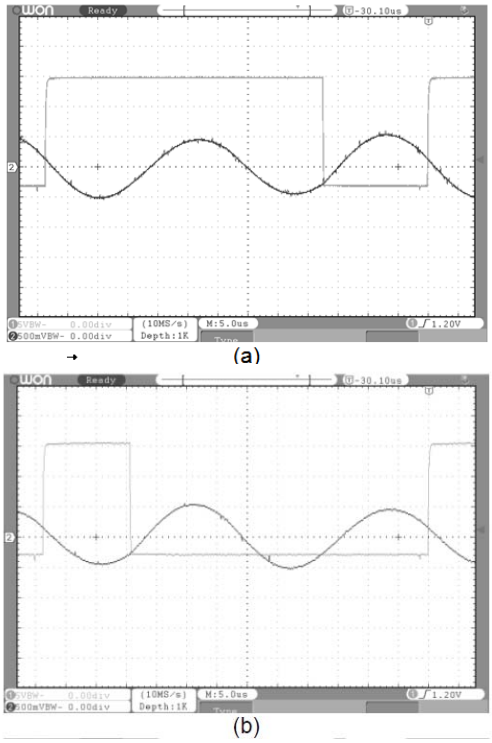
(a)

(b)

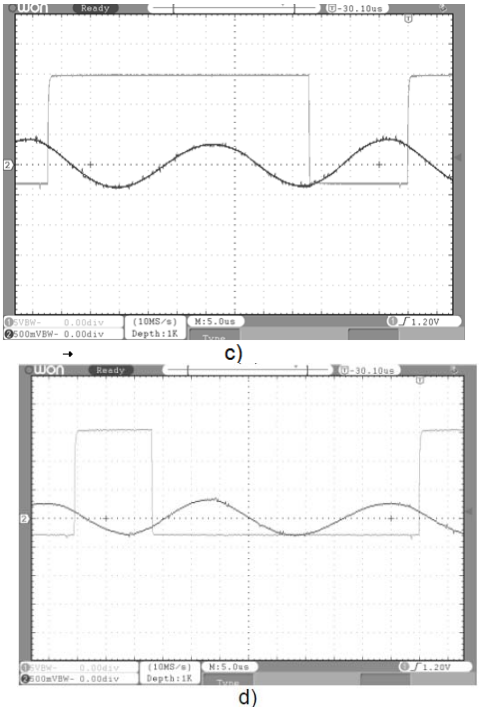

Fig. 12. Waveforms of the current i_O and the control signals of the transistors Q_1 and Q_4: a) Q_1 control signal in the case of $\phi = 0$; b) Q_4 control signal in the case of $\phi = 0$; c) Q_1 control signal in the case of $\phi > 0$; d) Q_4 control signal in the case of $\phi > 0$.

Also, Fig. 12 shows waveforms of i_O and the control signals of the transistors Q_1 and Q_4 in the case of $\phi > 0$. The experiments carried out fully confirmed the possibility of implementing the proposed combined PS-PDM control method for voltage-source series-resonant inverters for induction heating systems.

Conclusion

This paper has proposed a new control method for the series-resonant inverter of an induction heating system. The proposed combined PS-PDM control method of the SRI was explained. The main feature of this control method is that the current regulation for pulse density in the range from 0.5 to 1 is provided by only the traditional PDM control and in the range from 0 to 0.5 – with the PS control and constant density equal to 0.5 of the PDM control. Theoretical analysis shows that using the proposed control method can decrease the peak-to-peak current fluctuation up to 20% and increase the minimum peak current up to 12.2% at the quality factor of 5, compared with the traditional PDM control. The experimental waveforms obtained on an experimental setup have verified the feasibility of the proposed control.

***Author**: PhD Pavlo Herasymenko, Senior Researcher of Department of Transistor Converters, Institute of Electrodynamics of the National Academy of Sciences of Ukraine, 56 Peremohy Avenue, office 457, 03057, Kyiv, Ukraine, E-mail: herasymenko@ieee.org.*

REFERENCES

[1] Grajales L., Sabate J.A., Wang K.R., Tabisz W.A., Lee F.C., Design of a 10 kW, 500 kHz phase-shift controlled series-resonant inverter for induction heating, *1993 IEEE Ind. Appl. Conf. Twenty-Eighth IAS Annual Meeting*, (1993), 843-849

[2] Sawant R.R., Rao Y.S., A discrete-time controller for Phase Shift Controlled load-resonant inverter without PLL, *Proc. PEDES*, (2014), 1-4

[3] Nagai S., Michihira M., Nakaoka M., New phase-shifted soft-switching PWM high-frequency series resonant inverters topologies and their practical evaluations, *1994 Fifth Int. Conf. on Power Electron. and Var.-Speed Drives*, (1994), 274-279

[4] Uchihori Y., Kawamura Y., Tokiwa M., Kim Y.J., Nakaoka M., New induction heated fluid energy conversion processing appliance incorporating auto-tuning PID control-based PWM resonant IGBT inverter with sensorless power factor correction, *Proc. PESC '95*, (1995), 1191-1197

[5] Grajales L., Lee F.C., Control system design and small-signal analysis of a phase-shift-controlled series-resonant inverter for induction heating, *Proc. PESC '95*, (1995), 450-456

[6] Ibrahim O., Yahaya N.Z., Saad N., Phase-Shifted Full-Bridge Zero Voltage Switching DC-DC Converter Design with MATLAB/Simulink Implementation, *Int. Journal of Electr. and Comp. Eng.*, 8 (2018), No. 3, 1488-1497

[7] Kwon Y.S., Yoo S.B., Hyun D.S., Half-bridge series resonant inverter for induction heating applications with load-adaptive PFM control strategy, *Proc. APEC '99*, (1999), 575-581

[8] Fujita H., Akagi H., Pulse-density-modulated power control of a 4 kW, 450 kHz voltage-source inverter for induction melting applications, *IEEE Trans. on Ind. Appl.*, 32 (1996), No. 2, 279-286,

[9] Esteve V., et al., Using Pulse Density Modulation to Improve the Efficiency of IGBT Inverters in Induction Heating Applications, *2007 IEEE Power Electron. Specialists Conf.*, (2007), 1370-1373

[10] Sugimura H., Omori H., Lee H.W., Nakaoka M., PDM Controlled Series Load Resonant Soft Switching High Frequency Inverter for Induction Heated Toner Fixing Outer Roller with Inner Cylindrical Working Coil Stator, *2006 CES/IEEE 5th Int. Power Electron. and Motion Control Conf.*, (2006), 1-5

[11] Mucko J., The control methods of series resonant inverters which make possible the simultaneous work of transistors as the ZVS and the "almost ZCS" switches, Przeglad Elektrotechniczny, 86 (2010), No. 6, 137-142

[12] Pholsriphim A., Nurach S., Lenwari W., Half-bridge resonance inverter for induction heating using digital-controlled pulse density modulation technique, *Proc. ICIEA*, (2017), 1084-1086

[13] Herasymenko P.Y., A transistor resonant voltage inverter with pulse density modulation for induction heating equipment, *Technical Electrodynamics*, (2015), No. 6, 24–28

[14] Esteve V., et al., Enhanced Pulse-Density-Modulated Power Control for High-Frequency Induction Heating Inverters, *IEEE Trans. on Ind. Electron.*, 62 (2015), No. 11, 6905-6914

[15] Hu J., Bi C., Jia K., Xiang Y., Power Control of Asymmetrical Frequency Modulation in a Full-Bridge Series Resonant Inverter, *IEEE Trans. on Power Electron.*, 30 (2015), No. 12, 7051-7059

[16] Fan M., Shi L., Yin Z., Jiang L., Zhang F., Improved Pulse Density Modulation for Semi-bridgeless Active Rectifier in Inductive Power Transfer System, *IEEE Trans. on Power Electron.*, 34 (2019), No. 6, 5893-5902

[17] Zied H.A., Mutschler P., Bachmann G., A modular IGBT converter system for high frequency induction heating applications, *Proc. PCIM.*, (2002)

[18] Dede E.J., Jordan J., Esteve V., The practical use of SiC devices in high power, high frequency inverters for industrial induction heating applications, *Proc. SPEC*, (2016), 1-5

[19] Pinheiro J.R., Grundling H.A., Vidor D.L.R., Baggio J.E., Control strategy of an interleaved boost power factor correction converter, *30th Annual IEEE Power Electron. Specialists Conf. Record.*, (1999), 137-142

[20] Xu X., Liu W., Huang A.Q., Two-Phase Interleaved Critical Mode PFC Boost Converter with Closed Loop Interleaving Strategy, *IEEE Trans. on Power Electron.*, 24 (2009), No. 12, 3003-3013

[21] Herasymenko P., Yurchenko O., An Extended Pulse-Density-Modulated Series-Resonant Inverter for Induction Heating Applications, *Proc. RTUCON*, (2020), 1-8

[22] Shen J., Ma H., Yan W., Hui J., Wu L., PDM and PSM Hybrid Power Control of a Series-Resonant Inverter for Induction Heating Applications, *2006 1ST IEEE Conf. on Ind. Electron. and Applications*, (2006), 1-6

[23] Namadmalan A., Universal Tuning System for Series-Resonant Induction Heating Applications, *IEEE Trans. on Ind. Electron.*, 64 (2017), No. 4, 2801-2808